Defect production and annealing in ion-irradiated Si nanocrystals

D. Pacifici, E. C. Moreira, G. Franzò, V. Martorino, and F. Priolo
INFM and Dipartimento di Fisica e Astronomia, Corso Italia 57, I-95129 Catania, Italy

F. Iacona
CNR-IMETEM, Stradale Primosole 50, I-95121 Catania, Italy

(Received 7 November 2001; published 1 April 2002)

In this paper the formation and annihilation of defects produced in Si nanocrystals (nc) by ion-beam irradiation are investigated in detail. The luminescence properties of Si nanocrystals embedded in a SiO_2 matrix were used as a probe of the damaging effects generated by high-energy ion-beam irradiation. Samples have been irradiated with 2 MeV He^+, Si^+, Ge^+, and Au^+ ions at different doses, in the range between $1\times10^9/cm^2$ and $1\times10^{16}/cm^2$. With increasing the ion dose, the nc-related photoluminescence (PL) strongly decreases after a critical dose value, which depends on the ion mass. We have observed that the luminescence drop is accompanied by a concomitant lifetime quenching that marks the rise of new nonradiative phenomena, related to the damage left over by the ion beam. It is shown that the lifetime quenching alone cannot quantitatively explain the much stronger PL drop, but the total number of emitting centers has to diminish too. By assuming that a Si nc is damaged when it contains at least one defect inside its volume, we developed a model that relates the fraction of quenched nc to the total defect concentration in the film and to the value of the nc volume itself. This model is shown to be in good agreement with the experimental value of the quenched fraction of Si nc extracted from the luminescence and lifetime measurements. Moreover, we studied the recovery of the damaged Si nc by performing both isochronal and isothermal annealings. It is demonstrated that in slightly damaged Si nc a large variety of defects characterized by activation energies between 1 and 3 eV exists. On the contrary, the recovery of the PL properties of completely amorphized Si nc is characterized by a single activation energy, whose value is 3.4 eV. Actually, this energy is associated with the transition between the amorphous and the crystalline phases of each Si grain. The recrystallization kinetics of Si nanostructures is demonstrated to be very different from that of a bulk system. These data are presented and explained on the basis of the large surface/volume ratio characterizing low-dimensional Si structures.

DOI: 10.1103/PhysRevB.65.144109 PACS number(s): 78.55.−m, 61.72.Cc, 61.46.+w

I. INTRODUCTION

Since the discovery of porous silicon as an efficient light emitter,[1] a lot of work has been done in order to understand the origin of the peculiar luminescence properties of silicon nanostructures. Nowadays it is well understood that quantum confinement is responsible for the blue-shifted emission of these nanostructures and that the Si═O double bond at the interface between a Si nanocrystal and the oxide host plays a crucial role in explaining the strong Stokes shift between the emission and the absorption observed in porous Si, producing carrier-related states in the band gap from which the electron-hole (*e*-*h*) pair can recombine after being quickly trapped in. Moreover, the spatial confinement of carriers determines both a greater overlap of the *e*-*h* wave functions in *k* space and a strong suppression of nonradiative recombination processes, thus producing an increase of the luminescence efficiency. Among all, porous silicon,[1–4] silicon nanocrystals (nc) embedded within SiO_2 (Refs. 5–14) and Si/SiO_2 superlattices (SL's),[15–17] have been widely studied both from an optical and a structural point of view. In particular, it has been recently demonstrated that, in general, Si nc act as interacting systems within the oxide matrix, with the energy preferentially transferred from the smaller (i.e., larger band gaps) to the bigger ones (i.e., smaller band gaps).[5] This interaction can be strongly suppressed by ordering the Si nc in nanometric periodic layers, spaced by an oxide layer. In this way the energy hopping between nc is less probable, due to the larger mean distance among Si nc.[5]

The damage and recrystallization of crystalline bulk silicon is a well-known and widely studied subject.[18–24] Only recently the recrystallization properties of amorphous Si layers with thicknesses larger than 2 nm have been studied in greater details and the most important result is that the crystallization temperature increases with decreasing layer thickness.[25–27] In contrast, apart from a few papers,[28,29] the role of ion-beam-induced damage in the structural and optical properties of Si nanocrystals embedded in SiO_2 is not yet clear, and a comprehensive picture of the overall damaging mechanisms in Si nc is still lacking.

In the present paper the luminescence properties of Si nc produced by plasma-enhanced chemical-vapor deposition are used as a probe of the defect generation under irradiation through energetic ion beams. By varying both the dose and the mass of the incident ions, the main physical parameters responsible for the quenching of the photoluminescence have been determined. Moreover, the defect annihilation has been studied by observing the luminescence recovery after both isochronal and isothermal annealings. It is shown that a large variety of defects, having different activation energies, exists in partially damaged Si nc, while the recrystallization of fully amorphized Si nc is a thermally activated process, characterized by a unique activation energy of ~3.4 eV. A phenomenological model that is able to explain the overall experimental picture is presented.

II. EXPERIMENT

Samples were prepared by plasma-enhanced chemical-vapor deposition (PECVD) using high-purity SiH_4 and N_2O as precursors. The substrates, consisting of 5″ (100) Czochralski silicon wafers, were heated at 300 °C during the deposition process. The deposition system consists of a vacuum chamber (base pressure 1×10^{-9} torr) and a radio frequency (rf) generator (13.56 MHz), connected through a matching network to the top electrode of the reactor. The bottom electrode is grounded and acts also as sample holder.

We prepared two kinds of samples containing Si nanocrystals. The first one is a 0.1-μm-thick substoichiometric SiO_x ($x<2$) thin film with 39 at. % of Si. The deposition process was performed by using N_2O and SiH_4 as source gases, 50 W of rf input power, and a total pressure of 6×10^{-2} torr. After deposition, the SiO_x films were annealed for 1 h at 1250 °C in ultrapure nitrogen atmosphere. The high-temperature annealing induces the phase separation between Si and SiO_2 and a high density of small Si clusters is obtained,[5] with a mean radius of about (1.5 ± 0.4) nm.

The second kind of sample is a Si/SiO_2 superlattice, consisting of 11 SiO_2 layers (6.5 nm thick) alternated with ten ultrathin Si layers (0.9 nm thick). The SiO_2 layers were deposited by using a N_2O/SiH_4 mixture, with a total pressure of 3.5×10^{-2} torr and 30 W of rf power. Si layers were deposited by using SiH_4, with a total pressure of 1.5×10^{-2} torr and 25 W of rf power. After deposition, the SL's were annealed for 1 h at 1100 °C in ultrapure nitrogen atmosphere to induce the breaking and balling up of the ultrathin Si films, with the formation of Si nc totally embedded within SiO_2 and almost completely isolated, as demonstrated in previous works.[5,16]

In order to study the defect formation in Si nc, the samples were irradiated at room temperature with 2 MeV He^+, Si^+, Ge^+ or Au^+ ions at different doses in the range between 1×10^9 and $1\times10^{16}/cm^2$. The beam energy was chosen in order to locate the projected range beyond the films containing Si nc. In fact for all the used ions, the calculated projected range varies between 0.47 μm for Au and 6.84 μm for He. By changing the ion mass, the nuclear energy loss was varied over four orders of magnitude, in the range between 2.5×10^{-2} eV/Å for He and 2.6×10^2 eV/Å for Au. Through a detailed damage calculation by using the transport of ions in matter (TRIM) Monte Carlo simulations,[30,31] we calculated the area of each collision cascade. Moreover, the average number of displaced atoms per incident ion and per unit trajectory length has been evaluated within each cascade, and it varies in the range between 2.8×10^{-4} atoms/ion Å for He and 2.4 atoms/ion Å for Au.

Damage recovery of the as-implanted samples was performed by isochronal thermal annealings in the temperature range between 100 and 1150 °C in vacuum or in N_2 atmosphere. Moreover, in order to understand the kinetics of the damage recovery, we also performed isothermal annealings at different temperatures and for times in the range between 5 s and 20 h.

The structural and optical properties of all the samples have been studied by transmission electron microscopy (TEM) and photoluminescence, respectively. Dark field plan view and cross-sectional TEM analyses were carried out with a 200-kV Jeol 2010 FX microscope to determine the nanocrystal size distribution in both the damaged and the annealed samples.

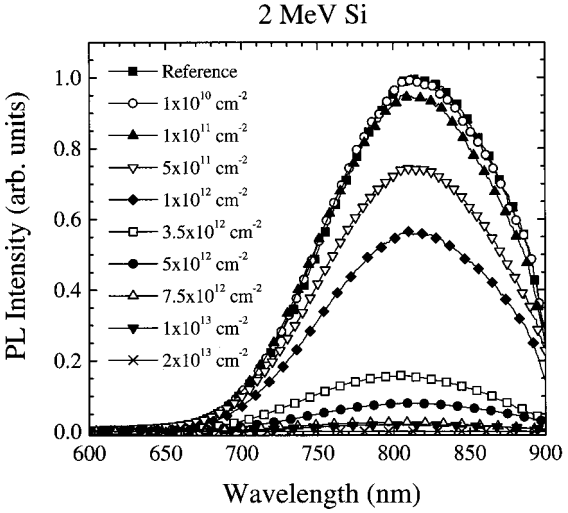

FIG. 1. PL spectra of a SiO_x film with 39 at. % Si annealed at 1250 °C for 1 h (reference) and of the very same sample irradiated with a 2 MeV Si^+ ion beam at different doses in the range between 1×10^{10} and $2\times10^{13}/cm^2$. Spectra were measured at room temperature, with the 488 nm line of an Ar-Kr laser as the exciting source and at a pump power of 10 mW.

Photoluminescence (PL) measurements were performed by pumping with the 488 nm line of an Ar-Kr laser. The pump power (10 mW) was focused over a circular area of ~0.6 mm in diameter and the laser beam was mechanically chopped at a frequency of 55 Hz. The luminescence signal was analyzed by a single grating monochromator and detected by a photomultiplier tube. Spectra were recorded with a lock-in amplifier using the chopper frequency as a reference. All the spectra have been measured at room temperature and corrected for the detector response. Luminescence lifetime measurements were performed by chopping the laser beam with an acousto-optic modulator, detecting the luminescence signal with the photomultiplier tube and analyzing it with a photon counting multichannel scaler having the signal from the modulator as a trigger. The overall time resolution of our system is of ~30 ns.

III. RESULTS AND DISCUSSION

A. Damage accumulation in Si nanocrystals

Before ion irradiation, all the samples show a strong photoluminescence even at room temperature. As an example, in Fig. 1 the PL spectrum of a sample containing Si nc (reference sample) obtained by annealing at 1250 °C a SiO_x film with 39 at. % of Si content is reported, together with the PL spectra of the same sample irradiated with 2 MeV Si^+ ions at different doses, in the range $1\times10^{10}-2\times10^{13}/cm^2$. The PL spectrum of the reference sample is peaked at 820 nm and has a full width at half maximum (FWHM) of about 140 nm. With increasing the ion dose, the PL intensity remains unaf-

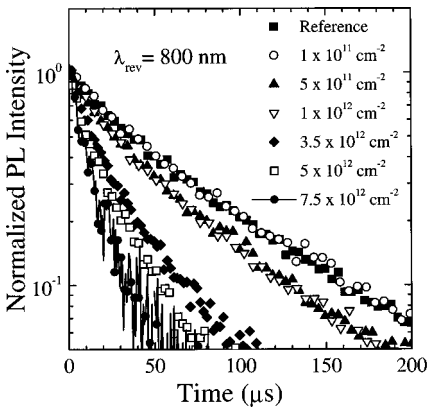

FIG. 2. Decay-time measurements of the photoluminescence signal at 800 nm for a SiO_x sample with 39 at. % Si, annealed at 1250 °C for 1 h (reference) and subsequently irradiated with 2 MeV Si^+ at different doses. Data were taken at room temperature and at a laser pump power of 10 mW. The measured lifetime for the reference sample is 54 μs.

fected up to $1\times10^{10}/cm^2$. For higher doses, the PL signal is clearly seen to decrease until it completely disappears for doses greater than $\sim1\times10^{13}/cm^2$. Neither shifts nor changes in the peak shape have been observed for all the used ion doses. Interesting information can be extracted by studying the decay time of the luminescence signal recorded at 800 nm after shutting off the pumping laser beam through the acousto-optic modulator, as reported in Fig. 2 for different ion doses. The luminescence signal decay is characterized by a stretched exponential shape, given by

$$I(t)=I_0\exp\left[-\left(\frac{t}{\tau}\right)^{\beta}\right], \tag{1}$$

where $I(t)$ and I_0 are the intensity as a function of time and at $t=0$, respectively, while τ and β are respectively the lifetime and a dispersion factor whose value gives an idea of the interaction strength among Si nc.[5,13,32] The lifetime values obtained by fitting the experimental curves reported in Fig. 2 with Eq. (1) remain constant up to a dose of $\sim1\times10^{11}/cm^2$, while they start to decrease for higher ion doses, suggesting that new nonradiative paths related to the presence of defects left over by the ion beam are influencing the decay dynamics of the emitting centers. On the other side, β is characterized by a value of 0.75, which remains constant for all the ion doses.

All the spectra and the decay time curves have been obtained with 10 mW of pumping power, resulting in a photon flux ϕ of about $8.7\times10^{18}\ cm^{-2}\,s^{-1}$. The Si nc excitation cross section σ is almost independent of the detection wavelength, i.e., of the Si nc size, and has a value of $\sim1\times10^{-16}\ cm^2$, as previously reported.[5] Thus, for the excitation rate of each Si nc we obtain a value $\sigma\phi\sim8.7\times10^2\ s^{-1}$, while the deexcitation rate for the reference sample is $\tau^{-1}\sim1.85\times10^4\ s^{-1}$ (τ being the luminescence lifetime of the reference sample, recorded at 800 nm). As $\sigma\phi\ll1/\tau$, we are in the low pump power regime. In this regime, which is valid for all the samples used, the PL intensity yield of the emitting centers can be approximated by the following expression:

$$I\propto\sigma\phi\frac{\tau}{\tau_R}N, \tag{2}$$

where τ_R is the radiative lifetime and N is the total number of Si nc that are able to emit. Equation (2) is extremely important for the understanding of the damaging mechanisms. In fact, it tells us that if the excitation conditions remain unchanged, a variation of the luminescence yield can be due only to a change in the lifetime τ or in the total number of emitting centers N, or in both of them. In Fig. 1 it is possible to observe that at a dose of $1\times10^{12}/cm^2$ the residual luminescence is ~60% of the reference one, while for the same dose the lifetime, reported in Fig. 2, is still ~80% of its original value. This means that in order to quantitatively explain the decrease of I through Eq. (2), the total number of emitting centers has to diminish too. In particular, it has to be about 75% of the total number of emitting centers present in the unirradiated sample. Thus we have an experimental evidence of the fact that even at very small doses (much smaller than the critical dose needed for the amorphization of bulk crystalline Si) we can damage Si nc in such a way that a fraction of them becomes ''dark'' from a luminescence point of view. These nc, however, though damaged, are not necessarily amorphized. In fact, from TEM analyses (not shown) it appears that even at a Si dose of $5\times10^{12}/cm^2$, a huge number of Si nc with the same size distribution as that of the reference sample is still visible in dark field configuration, while the PL signal reported in Fig. 1 is almost completely quenched, demonstrating that a Si nc can become ''dark'' without necessarily being amorphous.

We repeated the irradiation experiment on the very same sample by using several ions, at the same energy of 2 MeV. The results are shown in Fig. 3, where both the intensity and the lifetime of the PL signal at 800 nm coming from the irradiated sample are reported for different incident ions and versus the ion dose, normalized to the respective reference value. As can be seen, even if the range of doses varies over several orders of magnitude, due to the large spreading in the nuclear energy loss of the different ions, the general trend remains unchanged, with both the intensity and the lifetime strongly decreasing for doses greater than a critical value, depending on the particular ion used. In particular it is worth noticing again that for all the ions the luminescence intensity decreases more than the lifetime does with increasing the ion dose, confirming the fact that the total number of emitting Si nc is decreasing too. The picture that arises up to now is, therefore, the following: (1) with increasing the ion dose the total amount of damage left over by the ion beam in the matrix increases, the amount of damage being higher at a fixed dose for heavier ions; (2) the effect of damage is twofold, determining both the rising of new nonradiative paths, as attested by the decrease of the luminescence lifetime, and the reduction of the total fraction of emitting Si nc, both effects leading to a quench of the luminescence intensity in the irradiated samples. Thus for a fixed ion dose, we can

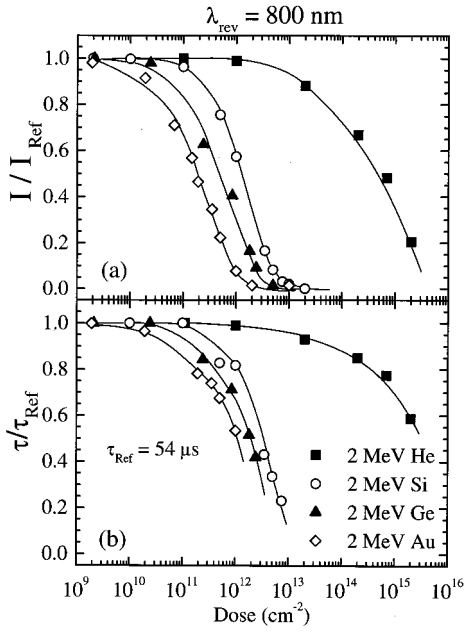

FIG. 3. Normalized PL intensities (a) and lifetimes (b) at 800 nm for a SiO_x film with 39 at. % of Si annealed at 1250 °C for 1 h and irradiated with 2 MeV He^+, Si^+, Ge^+, Au^+ at different doses. The lines are guides to the eye.

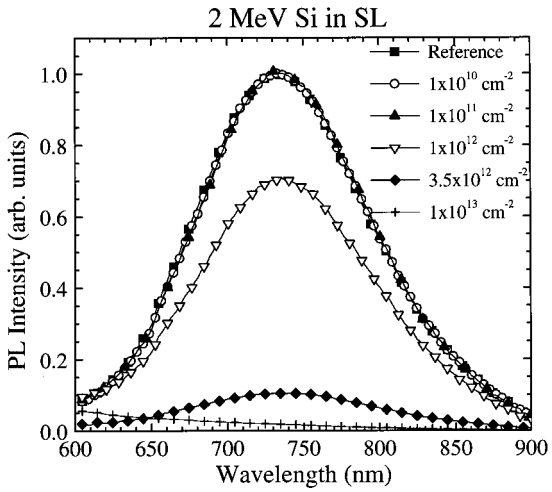

FIG. 4. PL spectra of a Si/SiO_2 superlattice (with a Si layer thickness of ~0.9 nm) annealed at 1100 °C for 1 h (reference) and after being irradiated with a 2 MeV Si^+ ion beam at different doses in the range between 1×10^{10} and $1\times10^{13}/cm^2$. Spectra were measured at room temperature and at a laser pump power of 10 mW.

think that the sample is composed of two different classes of Si nc, i.e., the first made of Si nc that cannot emit anymore, being damaged by the ion beam, the second formed of Si nc that can still emit but whose lifetime is strongly affected by new nonradiative processes.

In order to investigate the nature of these nonradiative phenomena, we produced a sample with largely spaced Si nc by annealing a Si/SiO_2 superlattice at 1100 °C for 1 h, as described in previous works.[5,16] The Si nc are located in parallel and far apart planes instead of being randomly and uniformly distributed all over the oxide host, and particular care was taken in order to obtain the very same Si nc size distribution. The sample was then irradiated with a 2 MeV Si ion beam, under the same experimental conditions. The PL spectra and the luminescence lifetime at 800 nm are respectively presented in Figs. 4 and 5. First of all it is worth noticing that, in spite of the same size distribution, the PL spectrum of the reference sample is blue-shifted with respect to the randomly distributed Si nc sample, being peaked at around 730 nm. Moreover, the lifetime of the same class of Si nc, i.e., those emitting at 800 nm, is different in the two reference samples, being longer and less stretched in the sample containing far apart Si nc. Both of these experimental evidences prove a strongly suppressed interaction among Si nc, which now act as to be almost isolated. It is interesting to note that in this sample though the PL intensity decreases with increasing dose (Fig. 4) the time decay remains constant, at least up to $1\times10^{12}/cm^2$. This demonstrates that, while the total number of luminescent centers is decreasing, no introduction of new nonradiative deexcitation paths is observed. The Si nc that can still emit seem to be unable to interact with the defects that are present in the oxide host after ion irradiation. The same must be true in the annealed SiO_x sample. So how do we explain the strong lifetime quenching in that sample? The Si nc concentration is higher, so that the mean distance between Si nc decreases, and a strong interaction among Si nc sets in. After ion irradiation, a nondamaged Si nc might be surrounded by a nearby damaged nc with whom it can interact. The damaged nc will, therefore, behave as a quenching center for the luminescing one, thus generating a nonradiative path for it. With increasing ion dose, the mean number of damaged nc surrounding a luminescent center increases, and so does the probability of a

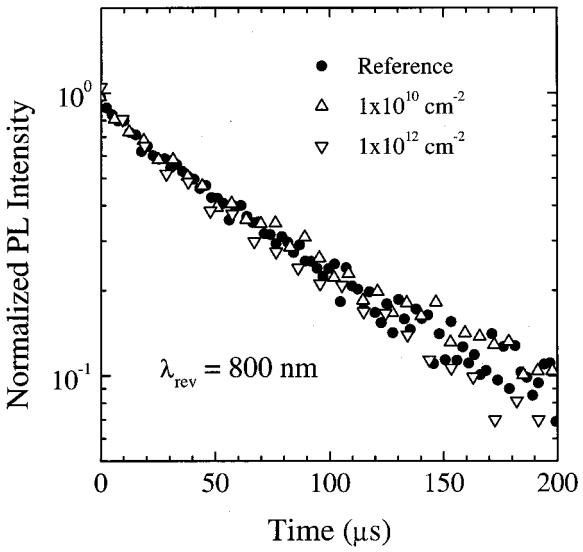

FIG. 5. Decay-time measurements of the PL signal at 800 nm for a Si/SiO_2 superlattice (with a Si layer thickness of ~0.9 nm) annealed at 1100 °C for 1 h (reference) and subsequently irradiated with 2-MeV Si^+ at different doses. Data were taken at room temperature and at a laser pump power of 10 mW. The measured lifetime for the reference sample is 63 μs.

nonradiative decay from the same nc, thus producing the lifetime quenching reported in Fig. 2.

B. Phenomenological modeling

It is well known that an energetic ion passing through a solid substrate can interact with a host atom by losing energy in electronic or nuclear collisions, being eventually stopped in the material. In the electronic stopping regime, the fast ion loses energy interacting with electrons in the solid, i.e., producing electronic excitations or ionizations of target atoms, while in nuclear stopping regime the ion loses much of its energy in an elastic collision with a host atom, eventually displacing it from its original lattice position if the lost energy is higher than a critical value, characteristic of the matrix and known as the *displacement energy*. If the displaced atom has enough energy, it can become itself a source of other displacements, thus producing a ''cascade,'' which is the spatial envelope of all the atoms displaced by both the primary and secondary ions. In our experiment we can assume that the energy of the incident ion is practically constant with depth, the film thickness being small ($\sim 0.1\ \mu$m) with respect to the projected range. This also means that within the film, each cascade can be approximated by a cylinder, whose height is the film thickness and whose area A_c can be defined as the area of a section perpendicular to the ion trajectory within which it is more probable to find a displaced atom. In order to determine the important parameters for the different collision cascades, we performed TRIM'90 Monte Carlo simulations[30,31] for the different ions at the irradiation energy. We thus obtained the total number of displaced atoms per incident ion within each cascade, for each ion mass, and the area A_c of each collision cascade. Once these parameters are known, it is easy to calculate the mean defect concentration n_c inside each collision cascade, defined as the ratio between the total number of displaced atoms D_c inside the cascade and the volume V_c of the cascade,

$$n_c = \frac{D_c}{V_c} = \frac{D_c}{A_c t} = \frac{d}{A_c}, \tag{3}$$

where t is the film thickness and $d \equiv D_c/t$ is defined as the number of displaced atoms per incident ion per unit trajectory length within each collision cascade. Thus the defect concentration in each collision cascade is just the number of displaced atoms per incident ion per unit length, divided by the mean cascade area.

Now we want to focus our attention on the defect formation within the Si nc dispersed in the SiO_2 matrix. We will assume that one single defect inside the volume of a nc is enough to quench its luminescence. This is plausible since, for instance, it has been demonstrated for porous Si that even a single Si dangling bond at the surface of a nanocrystallite acts as a very efficient nonradiative center, causing the complete quenching of the nc luminescence.[4] The fraction of quenched nc is, therefore, equal to the fraction of damaged nc, which is equal to the probability that a nc is damaged. In other words, we need to calculate the probability of finding at least one defect inside a nc, for a fixed ion dose ϕ. It is possible to distinguish between two different regimes for the ion dose, depending on the area of the collision cascade A_c. In fact, we can define a critical dose $\phi_c \equiv 1/A_c$, such that for $\phi \ll \phi_c$ we are in a first regime, characterized by very far apart collision cascades, while for $\phi \gg \phi_c$ a second regime arises, in which the collision cascades are completely overlapping.

In the first case a Si nc can be damaged only if it is located inside a cascade, all the defects being concentrated in that particular region of the film. But even if the nc is inside a cascade, this does not necessarily mean that it is damaged, as the location of a defect inside a cascade is a stochastic phenomenon. Thus, the probability P_d of a Si nc being damaged after ion irradiation at doses much smaller than the critical value must be the product of the probability P_c of finding the nc inside a cascade and the probability $P_{\geqslant 1}$ that, being inside the cascade, at least one defect is contained in its volume $V_{\rm nc}$. At a fixed ion dose ϕ, we can determine a surface of the film $S \equiv 1/\phi$ containing only one collision cascade. Since we are interested in the fraction of quenched nc, we can concentrate our analysis on the volume under this area S, which is representative of the overall film. The probability of a nc being in the volume of the collision cascade is simply given by

$$P_c = \frac{A_c}{S} = \phi A_c, \tag{4}$$

no matter at which depth it is located. Now we switch to the calculation of $P_{\geqslant 1}$, i.e., the probability that at least one defect exists inside a nc. First of all, it is necessary to calculate the probability of having exactly m defects inside a nc. The total number of defects M inside the cascade is given by $M = n_c V_c$, where n_c is the concentration of displaced atoms and $V_c = A_c t$ is the volume of the cascade. The probability of generating a defect exactly in the nc is given by

$$p = \frac{V_{\rm nc}}{V_c}, \tag{5}$$

where $V_{\rm nc}$ is the nc volume. Whilst the probability of a defect being located outside the nc is

$$q = 1 - p = 1 - \frac{V_{\rm nc}}{V_c}. \tag{6}$$

Thus, taking all the possible configurations into account, the probability of having exactly m defects in the nc and the remaining M-m outside its volume is given by the binomial distribution

$$P_m = \frac{M!}{m!(M-m)!} p^m q^{M-m}. \tag{7}$$

It is worth noticing that the mean number of defects contained in a nc is equal to

$$\overline{m} = pM = \frac{V_{\rm nc}}{V_c} n_c V_c = n_c V_{\rm nc}, \tag{8}$$

which is the defect density times the nc volume, as one would expect. Since $V_{nc} \ll V_c$, it results that $p \ll q$ and also $m \ll M$. Thus Eq. (7) can be approximated by the Poisson's normal distribution

$$P_m = \frac{\bar{m}^m}{m!} e^{-\bar{m}}. \tag{9}$$

In order to calculate the probability of having at least one defect inside the nc, we need to sum Eq. (9) over m in the range between 1 and M. Being $m \ll M$, we make a small error in summing between 1 and ∞. Thus we have

$$P_{\geqslant 1} = \sum_1^\infty {}_m P_m = \sum_0^\infty {}_m P_m - P_0 = 1 - P_0, \tag{10}$$

where we have used the normalization condition. P_0 is the probability that the nc has no defects at all, being therefore still ''alive,'' and is given by $P_0 = e^{-\bar{m}}$. Eventually,

$$P_{\geqslant 1} = 1 - e^{-\bar{m}} = 1 - e^{-n_c V_{nc}}. \tag{11}$$

Then the total probability that a nc is damaged by the ion irradiation and for a dose much smaller than the critical one, i.e., $\phi \ll \phi_c$, is

$$P_d = P_c P_{\geqslant 1} = \phi A_c (1 - e^{-n_c V_{nc}}). \tag{12}$$

It is worth noticing that the mean defect concentration N_d inside the film can be expressed as the ratio between the total number of displaced atoms in a cascade and the volume of the region of interest containing that cascade, having surface area S and thickness,

$$N_d = \frac{D_c}{St} = d\phi, \tag{13}$$

where we used again the definitions $S \equiv 1/\phi$ and $d \equiv D_c/t$. By using Eq. (13) together with Eq. (3), it is possible to rewrite Eq. (12) in the form

$$P_d = \frac{N_d}{n_c} (1 - e^{-n_c V_{nc}}). \tag{14}$$

Developing the exponential in terms of $n_c V_{nc} \ll 1$, Eq. (14) can be written in a first-order approximation as

$$P_d \cong N_d V_{nc}, \tag{15}$$

which shows that for $\phi \ll \phi_c$ and for cascades of low density the probability of damaging a nc varies linearly with the mean defect concentration N_d in the film, being independent of any parameter related to the particular ion used.

If $\phi \gg \phi_c$, the cascades are totally overlapping, thus all of the film surface is covered by the ion beam. Hence the probability P_c of finding a nc in a cascade is just 1. In this regime the probability P_d is determined only by the defect concentration N_d, which now increases linearly with ion dose and can be approximated by

$$N_d = n_c \frac{\phi}{\phi_c} = \frac{d}{A_c} \frac{\phi}{\phi_c} = d\phi, \tag{16}$$

where we used the definition $\phi_c \equiv 1/A_c$. Thus we regain the same result found in Eq. (13) for a completely different dose regime.

Therefore, the probability that a nc has at least a defect inside its volume can be easily obtained by substituting n_c with N_d in Eq. (11), thus resulting in

$$P_d = 1 - e^{-N_d V_{nc}}, \tag{17}$$

which tells us that the damage mechanism depends again only on the defect concentration N_d, i.e., through Eq. (16), on the number d of displaced atoms per incident ion per unit length, which is fixed by the matrix and the ion mass and energy, on the ion dose and on the nc volume. In particular, the smaller the nc volume, the higher has to be the ion dose in order to obtain the same fraction of damaged nc. Moreover, for a fixed nc volume and ion dose, the fraction of damaged nc depends only on d, i.e., on the ion mass and energy.

We previously assumed that a nc becomes ''dark'' when it contains at least one defect. Now it is easy to compare the model with the experimental data. By using Eq. (2) and the luminescence and lifetime data reported in Fig. 3, it is possible to obtain experimentally the quenched fraction f_q of Si nc, i.e., of nc that are unable to emit light after ion irradiation, versus the defect concentration related to the dose through Eq. (16), which is valid for all doses. In fact, we have

$$f_q = 1 - \frac{N}{N_{\mathrm{Ref}}}, \tag{18}$$

where N/N_{Ref} is the ''surviving'' fraction of Si nc, N is the number of still emitting centers after a certain dose ϕ and N_{Ref} is the total number of emitting Si nc in the reference sample, i.e., not yet irradiated. According to Eq. (2), N is proportional to the intensity I and inversely proportional to the luminescence lifetime τ. Thus, we easily obtain for the surviving fraction of Si nc,

$$\frac{N}{N_{\mathrm{Ref}}} = \frac{I}{I_{\mathrm{Ref}}} \frac{\tau_{\mathrm{Ref}}}{\tau}, \tag{19}$$

where all the variables are experimentally measurable. In Fig. 6 the experimental fraction of quenched Si nc, as determined through an analysis of the data shown in Fig. 3 by using formulas (18) and (19), is presented with different symbols for each ion and versus the defect concentration calculated through Eq. (16). In the same figure, the simulated curve of the damaged fraction of Si nc given by Eqs. (14) and (17) is reported as a continuous line (right-hand scale), by using a value of 1.7 nm for the mean Si nc radius, in good agreement, within the experimental errors, with the value determined by dark field TEM plan views. It is worth noticing that Eqs. (14) and (17) perfectly match at $N_d = n_c$. The impressive agreement between the experimental data and the simulated curve, in view of the fact that no adjustable param-

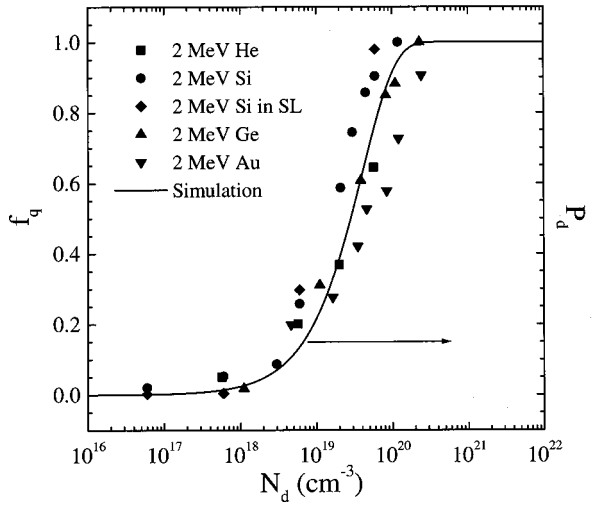

FIG. 6. Quenched fraction f_q of Si nanocrysals vs defect concentration N_d left over by the ion beam for a Si/SiO_2 superlattice (with a Si layer thickness of ~0.9 nm) annealed at 1100 °C for 1 h and after 2-MeV Si^+ implants (◆) and for a SiO_x film with 39 at. % Si annealed at 1250 °C for 1 h after 2-MeV He^+, Si^+, Ge^+, Au^+ implants (■, ●, ▲, ▼). The continuous line is the probability of a nc having at least one defect in its volume, as obtained from Eqs. (14) and (17) with the parameters fixed by the experiment.

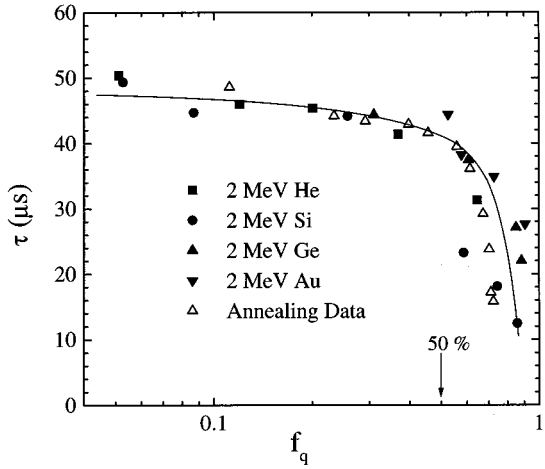

FIG. 7. Lifetime measured at 800 nm for a SiO_x film with 39 at. % Si annealed at 1250 °C for 1 h after irradiation with 2 MeV He^+, Si^+, Ge^+, Au^+ ions (■, ●, ▲, ▼) and for the same sample irradiated with 2 MeV Si^+ at a dose of $5\times10^{12}/cm^2$ after isochronal annealing processes at different temperatures in the range between 100 and 800 °C (△).

eters have been involved in the simulation, validates the hypothesis that in order to quench the nc luminescence, it is sufficient to have just one defect inside its volume. It is worth noticing that in the case of Si implants, i.e., fixing the *displacements per atom*, both the nc found in the annealed SiO_x sample and in the superlattice show the same experimental trend for the quenched fraction, even if their structure is very different.

We can gain a greater insight in the lifetime behavior of the irradiated Si nc formed in the annealed SiO_x film by plotting the luminescence lifetime at 800 nm versus the quenched fraction of Si nc, as reported in Fig. 7. It is interesting to observe that the lifetime has the same trend for all the ions used. This means that f_q is the right physical parameter to look at in trying to explain the quenching mechanisms occurring with increasing the ion dose. In particular for $f_q < 0.5$, the lifetime decreases only by a factor of ~0.8, while in the range $0.5 < f_q < 0.9$ it decreases very strongly, being reduced by a factor of ~0.2. In order to understand this experimental trend, at least qualitatively, we have first of all to stress the fact that the Si nc are interacting among each other. This interaction is reflected in the stretched exponential behavior shown by the luminescence decay time, which is characterized by a dispersion factor $\beta = 0.75$ for all the used ions. This factor gives an idea of the interconnection between nc, and tends to 1 when the nc are almost isolated. With increasing the ion dose and for all the ions used, β remains constant, demonstrating that the irradiation does not affect at all the energy transfer among neighboring nc. What the irradiation does is certainly to reduce the number of emitting Si nc, as previously demonstrated. In fact, with increasing defect concentration inside the film, more and more nc begin to contain at least one defect inside their volume, thus becoming damaged and, therefore, ''dark.'' But this does not prevent a damaged nc to interact with a good one. And, in fact, for a small fraction of damaged nc, i.e., small defect concentration N_d, the majority of nc are surrounded by non-damaged nc with which it can interact. So the energy can wander all around the sample until a damaged nc, acting as a nonradiative center, is met, thus causing the energy to be definitively lost. Increasing the fraction of quenched nc means to increase the total amount of quenching centers in the sample. In fact, this determines the slight decrease of the lifetime vs f_q (quenched fraction), which is experimentally observed for values up to 0.5. When f_q is equal to 0.5, this means that 50% of the total number of emitting centers is damaged, so that every emitting nc is surrounded by a damaged one. The vicinity between the emitting and the damaged centers causes the lifetime quenching to become much stronger. And, as a matter of fact, for $f_q > 0.5$ a quick drop in the luminescence lifetime is experimentally observed, as presented in Fig. 7. The behavior of τ for f_q values in the range between 0.9 and 1 is not experimentally accessible, since the luminescence signal of the irradiated samples is too feeble for lifetime measurements to be performed, but it would be reasonable to expect a saturation behavior for f_q approaching the value of 1. In fact, in this regime the few Si nc that are still able to emit are very far apart from one another, being completely surrounded by damaged nc. Thus adding one more damaged Si nc to the sample would not affect the lifetime properties of those emitting nc.

C. Defect annealing in Si nanocrystals

In order to investigate in greater detail the nature of the irradiation damage on Si nc, we annealed at different temperatures and for different times the Si nc, formed in the SiO_x film annealed at 1250 °C for 1 h and irradiated with 2

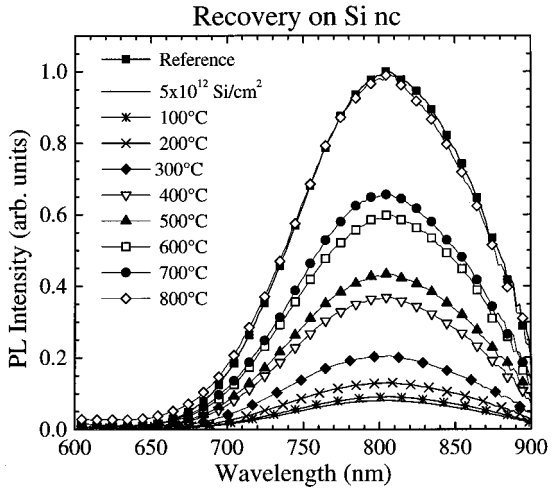

FIG. 8. PL spectra of a SiO_x film with 39 at. % Si excess annealed at 1250 °C for 1 h (reference), of the same sample after 2-MeV Si^+ irradiation at a dose of $5\times10^{12}/cm^2$ (continuous line) and of the irradiated sample after annealing processes for 4 h at different temperatures, in the range between 100 and 800 °C. Spectra were measured at room temperature and at a laser pump power of 10 mW.

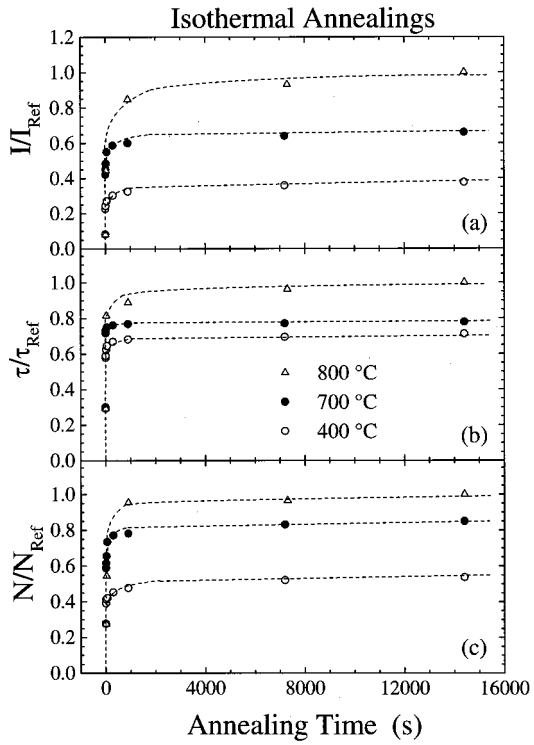

FIG. 9. Normalized PL intensities (a), lifetimes (b), and number of Si nc (c) emitting at 800 nm for a SiO_x film annealed at 1250 °C for 1 h, irradiated with 2-MeV Si^+ at a dose of $5\times10^{12}/cm^2$ and annealed at 400, 700, and 800 °C, for different times. The saturation behavior for each annealing temperature suggests the presence of many activation energies in the recovery process of damaged Si nc.

MeV Si^+ at a dose of $5\times10^{12}/cm^2$. At this dose, while a huge number of Si nc are still present in TEM dark field views, only 30% of the initial number of nc are surviving from a luminescence point of view. Therefore, this dose is enough to quench 70% of the initial number of Si nc without amorphizing them. In Fig. 8 the PL spectra of the as-implanted, of the reference, and of the samples annealed at different temperatures for 4 h, are shown. With increasing annealing temperature, the luminescence intensity is seen to increase, until it reaches the reference value at a temperature of 800 °C. No changes in the shape of the spectra have been observed within the temperature range used. The photoluminescence time decay curves recorded at 800 nm (not reported) show a complete recovery of the lifetime after annealing the sample at 800 °C too. This means that after an annealing at 800 °C for 4 h, also the number of emitting nc recovers its original value, attesting the fact that this thermal treatment is able to recover the damage in all the quenched Si nc.

At this stage a comment needs to be made. In Fig. 7 we showed that the lifetime of irradiated nc depends on the fraction of quenched Si nc and we explained this behavior in terms of energy migration among Si nc. If this is the case, a similar behavior should be obtained also after annealing. Indeed, in Fig. 7 the open symbols refer to the lifetime measured in annealed samples (at different temperatures) versus the fraction of quenched Si nc (which decreases with increasing the annealing temperature). The similar trend followed by the lifetime in both the irradiation and annealing experiments definitely demonstrates that the physical parameter that rules the quenching of the lifetime is just the fraction of quenched nc f_q, no matter how this value is obtained, whether through ion irradiation or by annealing of a damaged sample.

It is interesting to investigate the kinetics of both the intensity and the lifetime recovery, and eventually of the fraction of recovered Si nc. Thus we performed isothermal annealing processes for times between 5 s and 4 h, and for temperatures up to 1150 °C. As an example, in Fig. 9 the results obtained for three different temperatures (400, 700, and 800 °C) are reported. Both the intensity and the lifetime measured at 800 nm tend to quickly saturate for annealing times greater than ~10 s. The same trend is followed by the fraction of emitting nc, obtained through Eq. (19). It is worth noticing that for the two temperatures of 400 and 700 °C the saturation values are different, in particular the higher the temperature, the higher is the saturation value, but, more important, despite the long annealing times it is impossible to regain the initial value of emitting Si nc. This trend is typical of processes in which a continuous range of activation energies can take place. At each of the used annealing temperatures, a different set of annihilation processes is probed. Indeed for low temperatures, only those defects characterized by a low activation energy can annihilate at a measurable rate and when they are all removed a saturation is reached. At higher temperatures the processes with low activation energies have been completed, and only defects with progressively higher activation energies annihilate. Thus, the fact that at 800 °C after 4 h it is possible to obtain a total recovery of both the PL intensity and the lifetime, i.e., of the

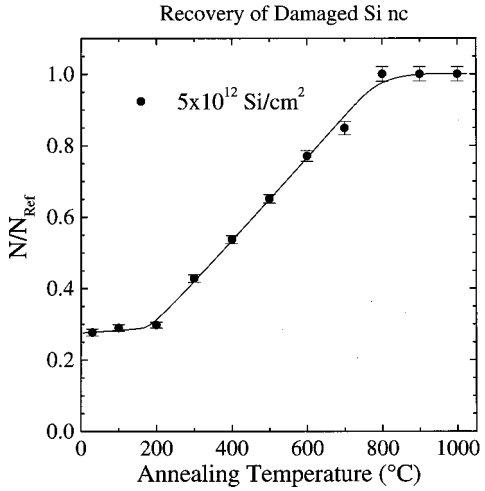

FIG. 10. Fraction of emitting Si nc in a SiO_x film annealed at 1250 °C for 1 h, irradiated with 2 MeV Si^+ at a dose of $5\times10^{12}/cm^2$ as a function of the annealing temperature. All the annealing processes were performed for 4 h, for which a saturation of both the intensity and the lifetime, i.e., of N/N_{Ref}, was observed. It is worth noticing that at 800 °C the complete recovery of the number of emitting Si nc occurs, thus fixing an upper limit for the activation energies characterizing the defects in the damaged Si nc.

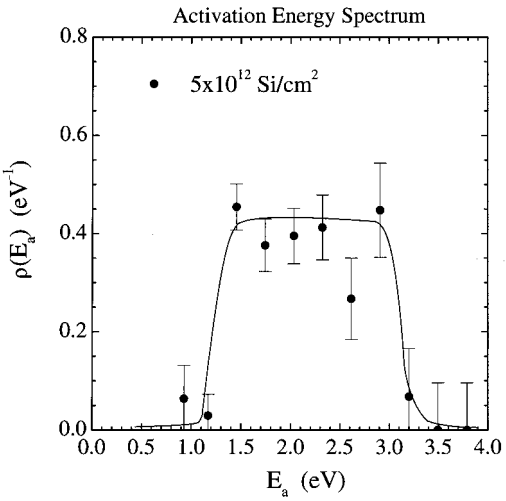

FIG. 11. Activation energy spectrum obtained for a SiO_x film with 39 at. % Si content annealed at 1250 °C for 1 h and irradiated with 2 MeV Si^+ at a dose of $5\times10^{12}/cm^2$. $\rho(E_a)$ is the derivative of N/N_{Ref}, shown in Fig. 12, with respect to the activation energy E_a related to the annealing temperature T through Eq. (20), and is proportional to the number of recovery events occurring per unit energy interval. The damaged Si nc are, therefore, characterized by a variety of defects with activation energies in the range between 1.5 and 3.0 eV.

fraction of emitting Si nc, means that an upper limit for the activation energies of the damaged sample exists.

It is possible to obtain the saturation value for the fraction of emitting nc vs the annealing temperature, by deducing it from the data in Fig. 8 and from the lifetime measurements through Eq. (19). The result of such an exercise is shown in Fig. 10. We want to stress the fact that the annealing time of 4 h is much higher than the saturation time of ~10 s, so that for each annealing temperature we are in an equilibrium regime. This means that in Fig. 10 we are looking at the total fraction of Si nc that can be recovered for each particular annealing temperature. At room temperature the surviving fraction of nc after the ion irradiation with a dose of $5\times10^{12}/cm^2$ is about 30% of the total number of emitting nc in the reference sample. Up to 200 °C, the population of damaged nc seems to be unaffected by the annealing. With increasing the temperature, the fraction of emitting nc starts to increase linearly, meaning that a certain number of defects are beginning to be annealed out. This linear regime ends at 800 °C, for which the damaged fraction of nc has totally been recovered.

More information can be obtained by a detailed analysis of the data shown in Fig. 10. In fact, from the data shown in Fig. 10, we can now obtain the activation energy spectrum of the defects present in Si nc. By fixing the annealing temperature we are selecting all those recovery events that involve the annealing of those defects with activation energies lower than a critical value E_a, related to that particular temperature by the well-known relation[33,34]

$$E_a = kT\ln(\nu t), \tag{20}$$

where k is the Boltzmann's constant, T is the annealing temperature in kelvin, $t\sim10$ s is the saturation value of the annealing time (see Fig. 9), and ν is an attempt frequency. Since we are involved in the annealing of defects in a crystalline matrix, we can assume that ν is the vibration frequency of an atom at that particular temperature, which is equal to $\sim kT/h$, where h is the Planck's constant. We can look at the distribution of recovery events by plotting the derivative of the emitting fraction of Si nc vs the activation energy given by Eq. (20), as reported in Fig. 11. This derivative, denoted as $\rho(E_a)$, represents the density of defect recovery events occurring per unit energy range. Hence $\rho(E_a)\Delta E$ gives the fraction of defects having activation energies in the range between E_a and $E_a+\Delta E$. The trend of $\rho(E_a)$ vs E_a reported in Fig. 11 is very interesting, as it demonstrates the presence of a population of defects in Si nc characterized by a continuous spectrum of activation energies, ranging between ~1 and ~3 eV. In particular, for $E_a<1.5$ eV, i.e., for temperatures lower than ~300 °C, practically no recovery events occur, while in the energy range between 1.5 and 3.0 eV, corresponding to the temperature range between 300 and 800 °C, a variety of defects that are annealed out at a constant rate exists in the low dose damaged nc.

A question now arises on the nature of the defects that we are producing and annihilating. At a Si dose of $5\times10^{12}/cm^2$ the collision cascades are overlapping, being $\phi>\phi_c$. Thus, through Eq. (8) in which we use for the defect concentration the value given by Eq. (13) instead of n_c, we can estimate the mean number of defects inside a nc to be ~1.2. In fact, for this value the surviving fraction of Si nc calculated by putting $m=0$ in Eq. (9) is just 30%. Moreover,

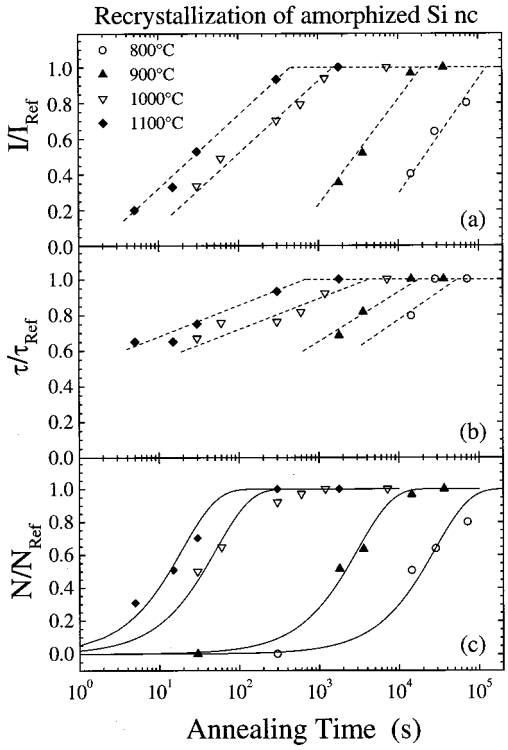

FIG. 12. Normalized PL intensities (a), lifetimes (b), and number of Si nc (c) emitting at 800 nm for a SiO_x film annealed at 1250 °C for 1 h, irradiated with 2 MeV Si^+ at a dose of $2\times10^{13}/cm^2$ and annealed at different temperatures in the range between 800 and 1100 °C and for different times. Dashed lines are guides to the eye, while continuous lines are fit to the data through Eq. (21). The PL properties as well as the crystallinity of the amorphized Si nc can be recovered at each of the annealing temperatures used, after an average annealing time τ_c that strongly depends on the particular temperature.

by using Eq. (9) we can calculate the probability of a nc having exactly *m* defects, or, which is the same, the fraction of nc containing in their volume exactly *m* defects, left over by the ion beam. In particular, the probability of having 1, 2, 3 or 4 defects in a nc is respectively equal to 0.36, 0.22, 0.09 or 0.03, the probability of having more than five defects being infinitesimal. Therefore, 36% of the damaged nc contain only one defect, while the remaining 34% have more than one defect inside. It is tempting to assume that the recovery events occurring with activation energies between 1 and 3 eV are related to the annihilation of defect structures whose variety and complexity increase with the number of defects actually present in each Si nc.

D. Recrystallization of amorphized Si nanocrystals

A totally different scenario is met by dealing with a Si nc sample irradiated with 2 MeV Si^+ ions at a dose of $2\times10^{13}/cm^2$. In fact at this particular dose the PL intensity is completely quenched, as can be seen in Fig. 1. This means that all the nc have been quenched. At the same time, in TEM dark field views (not shown), no more Si nc are present. Therefore, this low dose is enough to totally amorphize the Si nc present in the matrix. In order to study the recovery behavior of this system we performed thermal treatments of the as implanted sample at temperatures up to 1150 °C and for annealing times in the range between 5 s and 20 h. It has been observed that for temperatures up to 700 °C practically no recovery of the PL intensity is observed. In addition, no recrystallization occurred as seen by TEM. On the contrary, for temperatures higher than 700 °C something different occurs. As an example, in Fig. 12 the PL intensity, the lifetime and the number of nc emitting at 800 nm as obtained through Eq. (19), are reported, normalized to the respective values of the reference sample, versus the annealing time and for different annealing temperatures. As can clearly be seen, for each temperature, the PL intensity as well as the luminescence lifetime, measured at 800 nm, increase with increasing the annealing time, until they completely recover the reference values after a certain time that strongly depends on the particular annealing temperature. This behavior is also followed by the fraction of Si nc that are able to emit light again after the thermal treatments. Actually this fraction is equal to the fraction of recrystallized Si grains. In fact, after annealing at these temperatures, nc do appear again as observed by dark field TEM. Thus, by studying the recovery of the luminescence properties of the amorphized Si nc, we are indeed monitoring the transition between the amorphous and the crystalline phases of the Si grains present in the irradiated sample. The continuous lines in Fig. 12(c) are fit to the data by using the expression

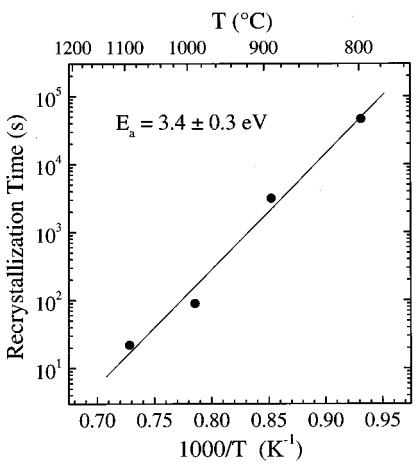

FIG. 13. The characteristic recrystallization time τ_c needed to completely recover the initial number of emitting Si nc, as extracted from the data in Fig. 12(c), is reported vs the reciprocal of the annealing temperature. An activation energy of 3.4 eV can be estimated for the recrystallization of amorphized Si nc.

$$\frac{N}{N_{\mathrm{Ref}}} = 1 - e^{-t/\tau_c}, \tag{21}$$

where τ_c is the characteristic crystallization time, strongly temperature dependent. As a matter of fact, by reporting in an Arrhenius plot (Fig. 13) this characteristic time (that is needed to attain the recovery of the Si grains) vs the reciprocal of the annealing temperature, we find that the recovery

process is thermally activated with a single activation energy of ~3.4 eV. Actually this is the activation energy for the recrystallization process of an amorphized Si nc.

A few comments need to be made at this stage. First of all, from the picture drawn up to now, it emerges that the complete amorphization of a Si nc can occur at doses as low as $2\times10^{13}/\mathrm{cm}^2$, at which it is estimated that only a few defects are left by the ion beam inside each nc. Since these doses are far away from the amorphization threshold of Si single crystal,[22,33] this demonstrates that amorphization of Si nc is by far easier than amorphization of bulk Si. This is not surprising. In fact, it is well known that the surface of a single-crystal Si wafer (i.e., its interface with the native oxide) represents a preferential nucleation site for amorphization[24] that starts there under ion bombardment well before than in the bulk. In the present case, each nc has a large surface area acting as a strong nucleation site for the amorphous phase.

Moreover, our data demonstrate that, while amorphization is easier in Si nc, crystallization is much more difficult with respect to a bulk amorphous Si. In fact, temperatures higher than 800 °C and long annealing times are needed to recrystallize the amorphized nc, the amorphous-to-crystalline phase transition being characterized by an activation energy of ~3.4 eV. This behavior is in agreement with recent data by Zacharias *et al.*,[27] showing that the crystallization temperature of very thin amorphous Si layers increases with decreasing layer thickness.

Indeed, we can think at the recrystallization of an amorphized Si nc as a transformation process occurring through nucleation and subsequent growth of the crystalline phase inside each nc, with the nucleation being the limiting step. Usually the homogeneous nucleation of the crystalline phase in an amorphous Si film is characterized by an activation energy of ~5.3 eV, as reported in Ref. 35. In our case, due to the large surface/volume ratio of each nc, the nucleation is probably heterogeneous, the surface being a preferential nucleation site. The activation energy of the nucleation process can be expressed as[35]

$$E_{a,\mathrm{nucl}}=\Delta G^{*}+E_{\mathrm{kinetic}}, \tag{22}$$

where ΔG^{*} is the free energy difference at the critical nucleus and E_{kinetic} the kinetic contribution, due to the formation and migration of the defects responsible for the phase transformation. In thermal nucleation ΔG^{*} is ~2 eV,[35] its value being determined by a balance between a free-energy reduction term due to the free-energy difference among the crystalline and the amorphous phases times the transformed volume, and a free-energy increase term due to the surface tension times the ''new'' surface formed as a result of the phase transformation. Since the nucleation occurs very likely at the surface of the amorphous zone, the ''new'' surface formed is much smaller and this results in a reduction in the surface-free-energy term and, in turn, in a dramatic reduction in ΔG^{*}. For instance, a surface reduction by a factor of 2 produces a decrease of ΔG^{*} by a factor of 8. We can then state that ΔG^{*} is probably small in the present case and most of the activation energy for the nucleation is due to the kinetic term. In fact, $E_{\mathrm{kinetic}}\sim3.4$ eV for amorphous Si (Ref. 35) actually equals the value we obtained for the activation energy associated to the recrystallization of amorphized nc.

Thus we would expect the crystallization of the amorphized nc to occur through nucleation followed by a rapid growth of the crystal grain. In fact, at 800 °C a few seconds are enough to totally grow a 1.5-nm Si nc using the literature growth velocities for small crystal grains.[35]

But, since the activation energy for nucleation is lower in amorphized nc than that in the bulk, why does the recrystallization of all the nc require such long times and high annealing temperatures? Actually, in order to attain the total crystallization of an amorphous bulk Si, only a few crystal nuclei need to be formed. In fact, subsequent growth of the crystalline phase is so fast that the total crystallization occurs in characteristic times that are much smaller than those required for the formation of new crystal nuclei. Therefore, the final structure consists of a few large grains. On the other hand, in order to observe the total recovery of the PL properties of the amorphized nc, all of them have to recrystallize. But the crystal growth is now spatially limited in the single grain volume, ending at the interface between the nc and the oxide matrix. Thus, in order to observe the complete recrystallization, we have to wait enough time for the nucleation to occur in ''all'' of the amorphous grains. As an example, in Ref. 35 it is reported that at ~800 °C the time needed for the total crystallization of the amorphous film is ~20 s. Since the measured nucleation rate is $\sim10^{13}/\mathrm{cm}^3$ s, this means that only $2\times10^{14}/\mathrm{cm}^3$ nucleation sites are formed, randomly distributed in the amorphous film. In our sample, the concentration of nc is $\sim10^{19}/\mathrm{cm}^3$, while the characteristic crystallization time at that temperature is $\sim5\times10^{4}$ s, bringing to a mean nucleation rate of more than $\sim2\times10^{14}/\mathrm{cm}^3$ s, i.e., one order of magnitude higher than for bulk amorphous Si. This increased value is a clear dimensionality effect present in our sample, arising from the high surface/volume ratio that characterizes the amorphized Si nc and favors the heterogeneous nucleation at the amorphized nc/SiO_2 interface. Despite the increased nucleation rate, the characteristic recrystallization times are much longer than for bulk amorphous Si, since we need to form a greater number of crystalline nuclei (i.e., at least equal to the total number of amorphized nc) and moreover in a well-defined region (i.e., in the Si nc volume).

IV. CONCLUSIONS

In the present work, the damaging effects of ion beam irradiation and subsequent annealing on Si nc have been reported. In particular, we used the luminescence properties of the irradiated and annealed nc as a probe of the damaging mechanisms occurring in Si nc. We demonstrated that by increasing the ion dose, the luminescence and the lifetime recorded at 800 nm begin to decrease after a critical dose depending on ion mass, the luminescence quenching being much stronger than the lifetime one. Thus, we have experimentally demonstrated that the number of emitting centers has to diminish too. This means that even at doses much lower than the one needed to amorphize bulk *c*-Si, a Si nc

can be damaged in such a way as to become ''dark'' from a luminescence point of view, not necessarily being amorphous. Anyway, by increasing the ion dose, a Si nc can even be amorphized at doses well below those needed to amorphize bulk crystalline silicon. By assuming that a Si nc remains damaged when it contains at least one defect, we developed a model in which the quenched fraction of nc depends exponentially on the nc volume and on the total defect concentration left over by the ion beam. The agreement with the quenched fraction of nc, extracted by the luminescence and lifetime measurements, demonstrates that it is sufficient to have just one defect inside the nc in order to quench its luminescence. Moreover, by performing isochronal and isothermal annealings of Si-irradiated samples, we were able to study in detail the recovery mechanisms in different dose regimes. We have demonstrated that at a Si dose of $5\times10^{12}/\mathrm{cm}^2$, corresponding to ~1 defect per nc on an average, defects are characterized by a large variety of activation energies in the range between ~1 and ~3 eV. In the case of amorphized nc, obtained at a Si dose of $2\times10^{13}/\mathrm{cm}^2$, the recovery process and consequently the transition between the amorphous and the crystalline phases of a Si grain, have been demonstrated to be thermally activated, with a single activation energy of ~3.4 eV, which has been directly associated with the nucleation process starting at the grain surface. Anyway, although it has been shown that nucleation rates one order of magnitude higher can be obtained due to surface effects, temperatures higher than 800 °C and longer annealing times are required with respect to bulk amorphous Si, in order for the recrystallization process to become measurable. In fact, while for amorphous Si only a few nuclei need to be formed, in order to observe the recrystallization of all the amorphized Si nc it is necessary to form a much larger number of nuclei, i.e., equal to the number of amorphous grains, and moreover, in a well-defined region, i.e., the grain volume. Thus the characteristic crystallization times become much longer than for amorphous Si. These data demonstrate that the amorphization of low-dimensional Si structures is much easier while crystallization is much more difficult with respect to bulk silicon.

ACKNOWLEDGMENTS

The authors wish to thank N. Marino, A. Marino, S. Pannitteri, and A. Spada for expert technical collaboration and A. Irrera for useful discussions. This work has been supported in part by the INFM Project RAMSES.

[1] L. T. Canham, Appl. Phys. Lett. **57**, 1046 (1990).
[2] M. V. Wolkin, J. Jorne, P. M. Fauchet, G. Allan, and C. Delerue, Phys. Rev. Lett. **82**, 197 (1999).
[3] A. G. Cullis, L. T. Canham, and P. D. J. Calcott, J. Appl. Phys. **82**, 909 (1997), and references therein.
[4] C. Delerue, G. Allan, and M. Lannoo, Phys. Rev. B **48**, 11 024 (1993).
[5] F. Priolo, G. Franzò, D. Pacifici, V. Vinciguerra, F. Iacona, and A. Irrera, J. Appl. Phys. **89**, 264 (2001).
[6] Y. Kanemitsu, T. Ogawa, K. Shiraishi, and K. Takeda, Phys. Rev. B **48**, 4883 (1993).
[7] T. Shimizu-Iwayama, K. Fujita, S. Nakao, K. Saitoh, T. Fujita, and N. Itoh, J. Appl. Phys. **75**, 7779 (1994).
[8] J. G. Zhu, C. W. White, J. D. Budai, S. P. Withrow, and Y. Chen, J. Appl. Phys. **78**, 4386 (1995).
[9] K. S. Min, K. V. Shcheglov, C. M. Yang, H. A. Atwater, M. L. Brongersma, and A. Polman, Appl. Phys. Lett. **69**, 2033 (1996).
[10] M. L. Brongersma, A. Polman, K. S. Min, E. Boer, T. Tambo, and H. A. Atwater, Appl. Phys. Lett. **72**, 2577 (1998).
[11] V. I. Klimov, Ch. Schwarz, D. McBranch, and C. W. White, Appl. Phys. Lett. **73**, 2603 (1998).
[12] T. Shimizu-Iwayama, N. Kunumado, D. E. Hole, and P. Townsend, J. Appl. Phys. **83**, 6018 (1998).
[13] J. Linnros, N. Lalic, A. Galeckas, and V. Grivickas, J. Appl. Phys. **86**, 6128 (1999).
[14] F. Iacona, G. Franzò, and C. Spinella, J. Appl. Phys. **87**, 1295 (2000).
[15] Z. H. Lu, D. J. Lockwood, and J.-M. Baribeau, Nature (London) **378**, 258 (1995); D. J. Lockwood, Z. H. Lu, and J. M. Baribeau, Phys. Rev. Lett. **96**, 539 (1996).
[16] V. Vinciguerra, G. Franzò, F. Priolo, F. Iacona, and C. Spinella, J. Appl. Phys. **87**, 8165 (2000).
[17] P. Photopoulos, A. G. Nassiopoulou, D. N. Kouvatsos, and A. Travlos, Appl. Phys. Lett. **76**, 3588 (2000).
[18] J. Dennis and E. B. Hale, J. Appl. Phys. **49**, 1119 (1978).
[19] F. F. Morehead and B. L. Crowder, Radiat. Eff. **6**, 27 (1970).
[20] O. W. Holland, S. J. Pennycook, and G. L. Albert, Appl. Phys. Lett. **55**, 2503 (1988).
[21] D. N. Seidman, R. S. Averback, P. R. Okamodo, and A. C. Baily, Phys. Rev. Lett. **58**, 900 (1987).
[22] S. U. Campisano, S. Coffa, V. Raineri, F. Priolo, and E. Rimini, Nucl. Instrum. Methods Phys. Res. B **80/81**, 514 (1993).
[23] G. L. Olson and J. A. Roth, Mater. Sci. Rep. **3**, 1 (1988).
[24] F. Priolo, A. Battaglia, C. Spinella, and E. Rimini, in *Surface Chemistry and Beam-Solid Interactions*, edited by H. Atwater, F. A. Houle, and D. Lowndes, MRS Symposia Proceedings No. 201 (Materials Research Society, Pittsburgh, 1991), p. 345.
[25] P. D. Pensans, A. Ruppert, and B. Abeles, J. Non-Cryst. Solids **102**, 130 (1988).
[26] M. Zacharias and P. Streitenberger, Phys. Rev. B **62**, 8391 (2000).
[27] M. Zacharias, J. Blasing, P. Veit, L. Tsybeskov, K. Hirshman, and P. M. Fauchet, Appl. Phys. Lett. **74**, 2614 (1999).
[28] G. A. Kachurin, M. O. Ruault, A. K. Gutakovsky, O. Kaitasov, S. G. Yanovskaya, and K. S. Zhuravlev, and H. Bernas, Nucl. Instrum. Methods Phys. Res. B **147**, 356 (1999).
[29] S. Cheylan, N. Langford, and R. G. Elliman, Nucl. Instrum. Methods Phys. Res. B **166–167**, 851 (2000).
[30] J. P. Biersack and L. G. Haggmark, Nucl. Instrum. Methods **174**, 257 (1980).
[31] J. F. Ziegler, J. P. Biersack, and U. Littmark, *The Stopping and Range of Ions in Solids* (Pergamon, New York, 1985).

[32] L. Pavesi, J. Appl. Phys. **80**, 216 (1996).
[33] S. Roorda, W. C. Sinke, J. M. Poate, D. C. Jacobson, S. Dieker, B. S. Dennis, D. J. Eaglesham, F. Spaepen, and P. Fuoss, Phys. Rev. B **44**, 3702 (1991).
[34] S. Coffa, F. Priolo, and A. Battaglia, Phys. Rev. Lett. **70**, 3756 (1993).
[35] C. Spinella, S. Lombardo, and F. Priolo, J. Appl. Phys. **84**, 5383 (1998).